Available online at www.sciencedirect.com

ScienceDirect

Procedia Structural Integrity 54 (2024) 99–106

Structural Integrity Procedia

www.elsevier.com/locate/procedia

International Conference on Structural Integrity 2023 (ICSI 2023)

Exploiting DIC-based full-field receptances in mapping the defect acceptance for dynamically loaded components

Alessandro Zanarini*

DIN, Industrial Engineering Dept., University of Bologna, Viale Risorgimento 2, 40136 Bologna, Italy

Abstract

Defect acceptance can be seen dependable upon the mapping of effective strains, due to dynamic loading of the components as they are mounted. With proper constitutive models and loading spectra, the experiment-based mapping of the equivalent stresses can be achieved from full-field receptances. Fatigue spectral methods turn this knowledge into components' life distributions, for the assessment of where the material reaches first the critical conditions for a failure, whereas can highlight areas of under utilization. Therefore, a risk grading mapping for potential defects can be formulated over the area of inquiry in order to discriminate among safe and dangerous locations. By following this experiment-based approach, potential defects in exercise and production might be tolerated in safer locations, under the chosen dynamic task, with great savings in costs and maintenance. Full-field dynamic testing can nowadays be achieved by means of optical measurements. Among the image-based ones, Hi-Speed DIC has proved to work in many environments, to be able to estimate full-field receptances of real components in their effective assembling and loading conditions also outside a specific laboratory. The quality achieved in the receptance maps helps in numerically deriving the strain FRFs on the sensed surface, to achieve, with known excitation, the experiment-based risk mapping of the real mounted component and defect acceptance criteria. Examples with coloured noises and a vibrating rectangular plate are highlighted in details.

© 2023 The Authors. Published by Elsevier B.V.
This is an open access article under the CC BY-NC-ND license (https://creativecommons.org/licenses/by-nc-nd/4.0)
Peer-review under responsibility of the scientific committee of the ICSI 2023 organizers

Keywords: defect acceptance; DIC-based dynamic testing; full-field FRFs; fatigue spectral methods; NDT.

1. Introduction

The key idea sketched in this brief article is to use a broad frequency band *experiment-based full-field FRF approach* to bring the complete & real structural dynamics into fatigue life expectations, which come as failure maps, therefore opening for a risk tolerance strategy of the defects that may be inside the material, due to the manufacturing process or to excessive loading during the service. In such a broad perspective, for the retained dynamics and for the high resolution mapping achievable, the location of the potential defect plays an uttermost relevance in the crack & failure start: what follows is devoted to highlight the potentials of this smart approach with simple examples from digital image correlation (DIC) optical (non-contact) full-field technique. The latter family of approaches can give:

* Corresponding author. Tel +39 051 209 3442.
E-mail address: a.zanarini@unibo.it (Alessandro Zanarini).

2452-3216 © 2023 The Authors. Published by ELSEVIER B.V.
This is an open access article under the CC BY-NC-ND license (https://creativecommons.org/licenses/by-nc-nd/4.0)
Peer-review under responsibility of the scientific committee of the ICSI 2023 organizers
10.1016/j.prostr.2024.01.061

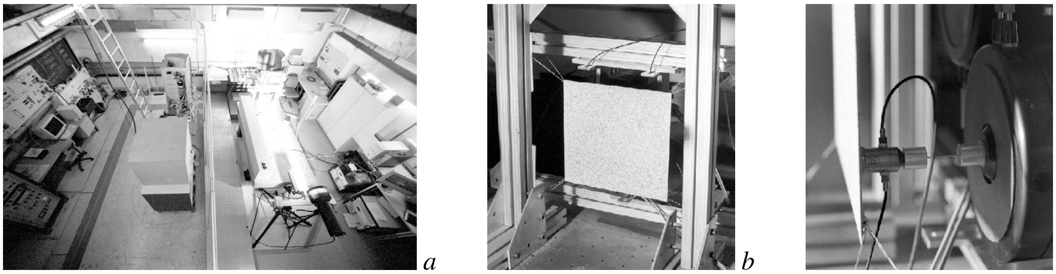

Fig. 1. The lab in the TEFFMA project: aerial view in *a*, restrained plate sample in *b*, 2 shakers on the back of the plate in *c*.

no structural dynamics distortions; a dense grid of sensing locations; a broad frequency band experimental vibration model, with accurate spatial description for complex pattern identification; an experimental dynamic model for strains (after numerical derivation), stresses & failure criteria; accurate maps of cumulative damage distributions for fatigue life assessment; defect tolerance criteria and risk index maps, dependable on excitation signature and location.

These works are spin-off activities rooting to the *Towards Experimental Full-Field Modal Analysis* (TEFFMA) project at TU-Wien, after the grown seeds put in the HPMI-CT-1999-00029 *Speckle Interferometry for Industrial Needs* Post-doctoral Marie Curie Industry Host Fellowship project at Dantec Ettemeyer GmbH. Since that testing (see Zanarini (2005b,a)) it became self-evident how full-field (ESPI) measurements could give relevant mapping about the local behaviour for enhanced structural dynamics assessments (see Zanarini (2007)) and fatigue spectral methods (see Zanarini (2008a,b)). The results in the former were the basis for the TEFFMA birth, whose works on SLDV, DIC & ESPI techniques saw earlier presentations in Zanarini (2014a,b), followed by Zanarini (2015b,a,c,d). In Zanarini (2018) a gathering of the works of TEFFMA was firstly attempted, while in Zanarini (2019a) an extensive description of the whole receptance testing was faced and in Zanarini (2019b) the EFFMA was detailed together with model updating attempts. The works in Zanarini (2020) underlined the quality of the datasets in full-field dynamic testing. The same quality inspired in Zanarini (2022d, 2023a,b) the sound propagation simulation by means on Rayleigh integral approximation. In Zanarini (2022b) a precise comparison was made about new achievements for rotational and strain FRF high resolution maps. In Zanarini (2022c,a, 2023c) the risk grading concept was first introduced by the exploitation of ESPI datasets, which are, contrary to DIC here used, difficult to be deployed outside a laboratory.

A brief description of the testing is outlined in Section 2, with attention on the set-up, on the used gears and on the obtained raw results. Section 3 deals with the numerical derivation of strain and stress fields from receptance maps, which are relevant to the cumulative damage spectral methods in Section 4. Section 5 pertains the selection of a defect tolerance scheme and its evidences with DIC-based *receptances*, before the final conclusions in Section 6.

2. The testing for the TEFFMA project in brief

To the interested reader, the most detailed notes on the test campaign appeared in Zanarini (2019a), with further suggestions in Zanarini (2019b, 2020, 2022b), but here is a brief summary of what was available at TU-Wien as in Fig.1: a dedicated seismic floor room; a mechanical & electronic workshop with technicians; traditional tools for vibration & modal analysis; but, in particular, there were SLDV, Hi-Speed DIC and ESPI measurement instruments.

2.1. Setting-up the rig for concurrent measurements

Accurate studies were needed to understand each technological limit and if a common test for concurrent usage might have been really possible. All this brought to a unique set-up for the comparison of the 3 optical technologies in full-field FRF measurements; great attention was paid on the design of experiments for further research in modal analysis. After an accurate tuning, a feasible performance overlapping was sought directly out of each instrument, reminding that the same structural dynamics can be sensed in complementary domains, which means frequency for SLDV & ESPI, time for DIC. The comparisons of the Operative Deflection Shapes, directly out of each instrument proprietary software, seem really promising, but only qualitative, as nothing is precisely super-imposable. A topology transform methodology is needed for quantitative comparison in the same physical locations of the specimen.

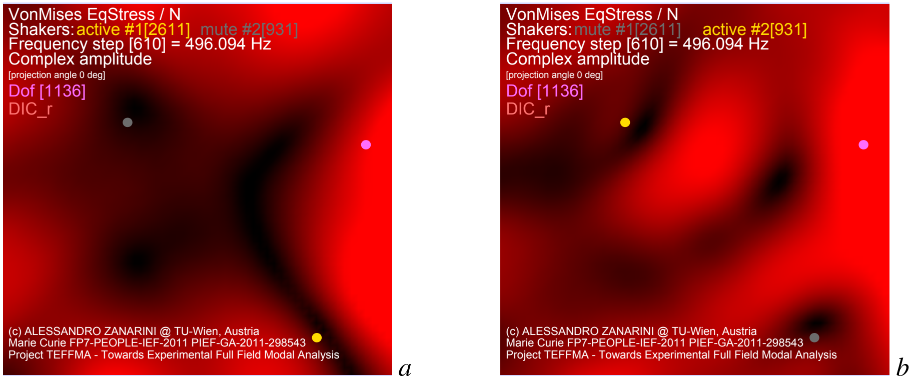

Fig. 2. Examples of *von Mises equivalent stress FRF maps* from optical techniques, direct experimental impedance models at 496 Hz, DIC examples: from shaker 1 in *a*, from shaker 2 in *b*.

2.2. *Estimated full-field FRFs & Coherence from optical measurements*

Once the methodology above is defined, *receptance FRF & Coherence function's* maps at specific frequencies and excitation sources can be obtained as in Zanarini (2019a), to appreciate the spatial consistency & continuity of the data, with clean shapes, sharp nodal lines and excellent *Coherences*, especially from ESPI. Each of the transformed dataset is precisely comparable with the others, up to the numerical precision of the topology transforms.

3. Deriving new quantities from full-field receptances

The high quality of these *receptance maps*, also obtainable from DIC, deserves further investigations for novel derivative quantities, starting from highly detailed strain maps.

3.1. *Dynamic Strain FRFs*

By means of a robust differential operator (see in particular Zanarini (2022b)) on the *receptance map* $\mathbf{d}(x, y, j\omega)$ along x & y directions, the *full-field generalised strain FRFs* can be obtained in each map location and frequency line:

$$\varepsilon(x, y, j\omega)_{ik} = \frac{1}{2}\left(\frac{\partial \mathbf{d}(x, y, j\omega)_i}{\partial q_k} + \frac{\partial \mathbf{d}(x, y, j\omega)_k}{\partial q_i}\right), \tag{1}$$

as well as the *strain tensor* components due to out-of-plane bending-related displacements of the plate of thickness s:

$$\varepsilon(x, y, j\omega)_{xx_b} = -\frac{s}{2}\frac{\partial^2 \mathbf{d}(x, y, j\omega)_z}{\partial x^2},\ \varepsilon(x, y, j\omega)_{yy_b} = -\frac{s}{2}\frac{\partial^2 \mathbf{d}(x, y, j\omega)_z}{\partial y^2},\ \gamma(x, y, j\omega)_{xy_b} = \gamma(x, y, j\omega)_{yx_b} = -s\frac{\partial^2 \mathbf{d}(x, y, j\omega)_z}{\partial x \partial y}. \tag{2}$$

Also the *Principal Strain FRF maps*, from both shakers, can be obtained at each frequency line of the domain, with a complex-valued data representation, to retain any phase relation: it becomes an impressively adherent characterisation of the experiment-based strain distribution over the sensed surface in spatial and frequency domains.

3.2. *Dynamic Stress FRFs*

With the introduction of a linear isotropic constitutive model (with the following material parameters: E elastic modulus, ν Poisson ratio, G shear modulus, Λ Lamé constant, here of the aluminium sample in Fig.1*b*,), the *Stress*

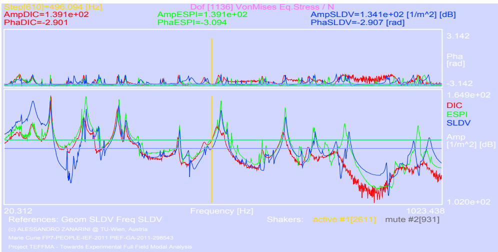 *a*

 *b*

Fig. 3. Examples of *von Mises equivalent stress FRF graphs* from optical techniques, direct experimental impedance models in the 20-1024 Hz range, DIC-ESPI-SLDV examples: from shaker 1 in *a*, from shaker 2 in *b*.

FRF tensor components can be evaluated from *Strain FRFs*:

$$\begin{aligned}\sigma_\omega(x,y)_{ii} &= 2G\varepsilon_\omega(x,y)_{ii} + \Lambda\left(\varepsilon_\omega(x,y)_{xx} + \varepsilon_\omega(x,y)_{yy}\right);\\ \sigma_\omega(x,y)_{ij} &= 2G\varepsilon_\omega(x,y)_{ij}; G = E/2\,(1+\nu); \Lambda = E\nu/((1+\nu)\,(1-2\nu)).\end{aligned} \tag{3}$$

Therefore, with the constitutive model of any specific material (anisotropic and locally linearised included), also the *experiment-based Principal Stress FRF maps* can be evaluated from the *full-field receptance* $\mathbf{d}(x, y, j\omega)$.

4. Cumulative damage & fatigue life assessment by means of spectral methods

With such a broad set of detailed *experiment-based Stress FRF maps*, we can evaluate cumulative damage with the *spectral methods* for high cycles fatigue in every dof of the sensed surface, with *unprecedented mapping abilities*. A spectral method targets the evaluation of an *equivalent range of stress cycles* $S_{eq}(x, y)$, in each location (x, y) of the *experiment-based Stress FRF maps*, representative of the damage inferred by the whole spectrum of the retained dynamics on all the locations of the sensed surface. The notation (x, y) is used for the spatial extension to maps.

Many *spectral methods* are based on $m_k = \int_0^\infty f^k PSD_{VM}(\omega)d\omega$, the *k-th order moments* of the frequency by the *power spectral density (PSD)* of *von Mises equivalent stress* $PSD_{VM}(\omega)$, from which we can obtain other parameters, such as the *effective frequency* $F_{zerocrossing} = F_{zc} = \sqrt{m_2/m_0}$, the *expected number of peaks per unit time* $F_{peaks} = F_p = \sqrt{m_4/m_2}$, and the *irregularity factor* $\gamma = \gamma_2 = F_{zc}/F_p = m_2/\sqrt{m_0 m_4}$.

4.1. Dirlik semi-empirical spectral method parameters

Among the many available (see Dirlik and Benasciutti (2021); Zorman et al. (2023)), the *Dirlik semi-empirical spectral method* in Dirlik (1985) was here implemented, as it gives a sound prediction of the fatigue life for wide-

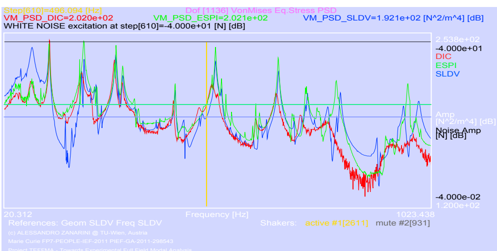 *a*

 *b*

Fig. 4. Examples of *white noise von Mises equivalent stress PSD* graphs from optical techniques, direct experimental impedance models in the 20-1024 Hz range, DIC-ESPI-SLDV examples: from shaker 1 in *a*, from shaker 2 in *b*.

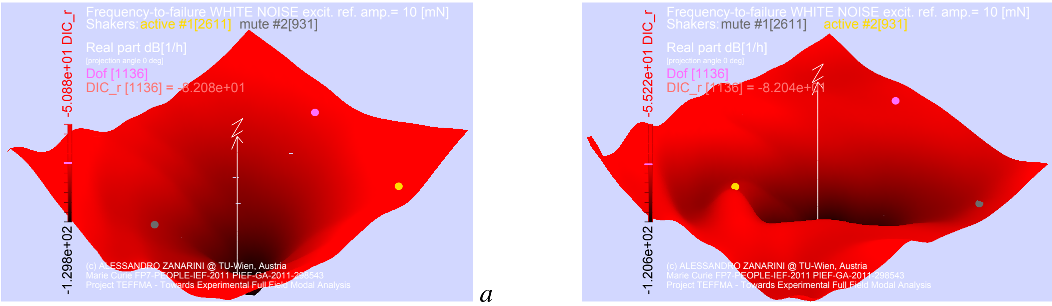

Fig. 5. Examples of *frequency-to-failure distribution* maps from *white noise excitation*, DIC examples: from shaker 1 in *a*, from shaker 2 in *b*.

frequency-band spectra of stress responses, combining the factors in Eq.4:

$$\begin{aligned}
&\chi_m = (m_1/m_0)\,(m_2/m_4)^{1/2}\,; D_1 = 2\left(\chi_m - \gamma^2\right)/\left(1+\gamma^2\right); R = \left(\gamma - \chi_m - D_1^2\right)/\left(1 - \gamma - D_1 + D_1^2\right)\\
&D_2 = \left(1 - \gamma - D_1 + D_1^2\right)/\left(1 - R\right); D_3 = 1 - D_1 - D_2; Q = 1.25\left(\gamma - D_3 - D_2 R\right)/D_1;
\end{aligned} \tag{4}$$

to finally obtain, in each location (x, y), the *Equivalent Range of Stress Cycles* S_{eq} raised to b exponent

$$S_{eq}^b = D_1(2\sqrt{m_0}Q)^b\Gamma(b+1) + (2^{3/2}\sqrt{m_0})^b\Gamma(1+b/2)[D_2R^b + D_3], \tag{5}$$

and the *Time-to-Failure spatial distribution* $T_{failure}(x, y)$, evaluated across all the dofs (x, y) of the maps, function of $S_{eq}(x, y)$, of $F_p(x, y)$ and of the K_r fatigue strength coefficient and b exponent, as:

$$T_{failure}(x, y) = K_r/\left[F_p(x, y)S_{eq}^b(x, y)\right]. \tag{6}$$

4.2. The role of von Mises equivalent stress FRFs from optical techniques

The *PSD of von Mises equivalent stress* is crucial and evaluated from the *von Mises equivalent stress FRFs*, here rendered in the maps at a single frequency in Fig.2 and in single dof graphs of Fig.3, from both shakers.

Important to note is that the *experiment-based full-field stress FRFs*, with their *principal components*, are usable with any other spectral method (see e.g. Dirlik and Benasciutti (2021)), in particular those that retain the phase relations in the frequency domain, for further comparative works.

4.3. Frequency-to-failure with coloured noise excitation

As in Zanarini (2015c, 2018, 2022c) new *PSDs* are easily obtained from the *stress FRFs*, when changing the *excitation signature* $F(\omega)$ and *energy injection point* (or shaker). By selecting the *white noise* excitation (in the shape of $F(\omega) = F_0/\omega^\alpha$, $\alpha = 0$, $F_0 = 0.01N$) to multiply the previous *stress FRFs*, the *PSDs* of *von Mises equivalent stress maps* (shown in single dofs in Fig.4) are used to give the reciprocal of Eq.6, what can be called the *frequency-to-failure*, to highlight where the failure should start first, as in Fig.5 by brighter red tones on higher log Z axis.

5. Defect tolerance based on full-field dynamic testing & Risk Index

With the *experiment-based Time-to-Failure maps* of Eq.6 a *defect tolerance criterion* can be built, in manufacturing as well as in exercise, based on the real dynamics and a *Risk Index* definition of our choice. Starting from the predictions by means of the *fatigue spectral methods* on experimental full-field data, an example of ***Risk Index*** can be proposed, which is based on the *Hours-to-Failure (HtF)* (instead of seconds as in Eq.6), and can be defined in every dof, in a decibel shape, relative to the *mean* of the *HtF* distribution:

$$RiskIndex_{[dof]} = RI_{[dof]} = 20log_{10}(\frac{1}{HtF_{[dof]}}) - 20log10(\frac{1}{HtF_{mean}}). \quad (7)$$

The *defect tolerance* can be said, therefore, as proportional to the defined *Risk Index*, putting a *Threshold-of-Acceptance (ToA)*: **defect tolerance** α **RI**, e.g. safety achieved when $RI \leq ToA$. Once the *ToA* is defined, a clear grading of the *RI* is achieved. A new color coding of the *RI* maps, introduced in this work, presents red tones for DIC, with increasing brightness related to the *RI* value up to the *ToA*, used as the switch to grey tones till the pure white of the maximal *RI* value; it becomes trivial to separate safe areas (in red) from dangerous ones (in grey), therefore assessing where a potential defect may be tolerated and where not.

The concept can be further expanded by any different *coloured noise excitation* $F(\omega)$, or also by *in-field measured forces*, to evaluate the related *von Mises equivalent stress PSDs*. Different *PSDs* bring their respective *Risk Index maps*. In the examples of Fig.6 the location of the magenta dof, with a *ToA* of 11 in Eq.7, gives the information if, according to the proposed *Risk Index* and the shaker's input location, the potential defect is tolerable or not, with clear safety repercussions in production or exercise. The examples of Fig.7, obtained instead with a *pink noise excitation* from both shakers, show completely different *Risk Index maps*, due to the lower emphasis on higher frequency contributions. This to underline the effectiveness of *full-field FRF based Risk Index mapping*: it was sufficient to change the *dynamic signature* of the excitation, and its location, to understand how the problematic (grey) areas on the sample changed.

The *damage location assessment* on real components may play a relevant role under the *defect tolerance strategies*. The chosen Figs.6-7 above were just virtual examples, but the same ESPI-based *NDT* shown in paper Zanarini (2022f) may give us a *real defect distribution map*, which can be the input in *Risk Index maps*, here obtained by DIC full-field dynamic testing (ESPI in Zanarini (2022e)), both for production & exercise of our parts. In this coupled strategy, the real location of the defect on the map can tell if it can be accepted (red tones) or not (grey tones), in manufacturing or exercise, once the real structural dynamics and excitation signature are fully known without simplifications. Therefore the *NDT*, the *structural dynamics'* measurement and the *defect tolerance criteria* can all be based on *full-field dynamic testing*, to put the most advanced experimental structural dynamics' knowledge into higher safety targets.

6. Conclusions

This brief paper has shown how a methodologically sound *risk tolerance assessment* can be run also on *DIC-based full-field FRFs*, which have less restraints than those from the ESPI approach. It was therefore possible to run the

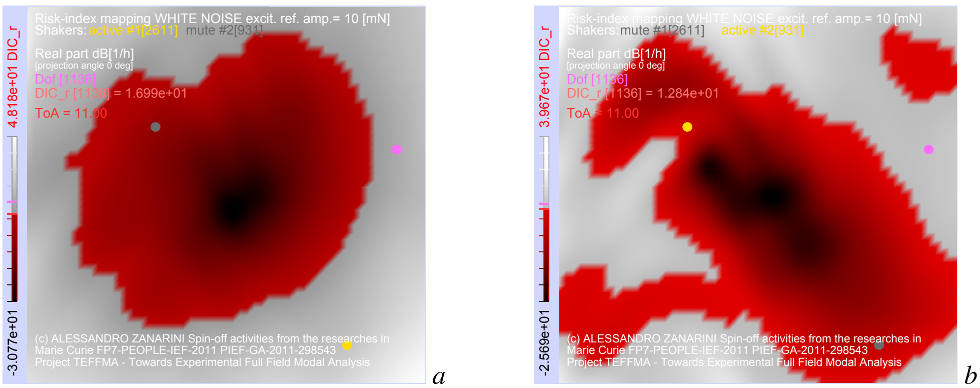

Fig. 6. Examples of *Risk Index mapping* in dof 1136, with *white noise excitation* from shaker 1 in *a* and shaker 2 in *b*. If *ToA=11*, a defect in dof 1136 is intolerable, thus dangerous, with both energy injection points.

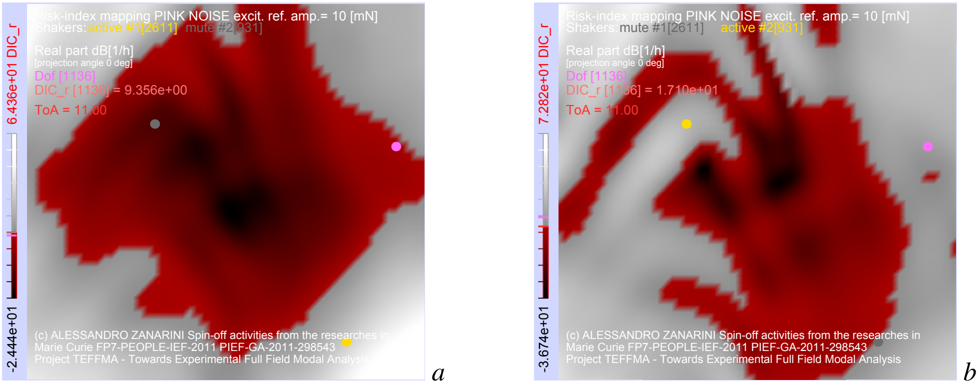

Fig. 7. Examples of *Risk Index mapping* in dof 1136, with *pink noise excitation* from shaker 1 in *a* and shaker 2 in *b*. If *ToA=11*, a defect in dof 1136 is tolerable when the excitation comes from shaker 1, whereas is intolerable, thus dangerous, if shaker 2 gives the excitation.

accurate evaluation of *Strain FRF maps*, of *Stress & von Mises equivalent stress FRF maps* with proper constitutive models, of *von Mises PSDs* directly from *experimental DIC-based full-field FRFs* and *coloured noise excitation*, of the *fatigue life predictions* by means of *spectral methods*, and of the *Risk Index maps*, to grade the dangerous location of defects with defined threshold of acceptance and related colour coding, once the real dynamic behaviour is fully retained and not simplified.

Experimental optical full-field measurement techniques, also in the DIC variant, are becoming mature & reliable for a *risk tolerance assessment* in production and working conditions, because of their ability to identify defects and to retain a refined and dense structural dynamics in both the frequency and spatial domain, directly from real samples and without any FE model to be carefully updated.

Acknowledgements

The European Commission Research Executive Agency is acknowledged for funding the project TEFFMA - Towards Experimental Full Field Modal Analysis, funded by the European Commission at the Technische Universitaet Wien, Austria, through the Marie Curie FP7-PEOPLE-IEF-2011 PIEF-GA-2011-298543 grant in years 2013-2015.

References

Dirlik, T., 1985. Application of computers in fatigue analysis. Ph.D. thesis. University of Warwick. URL: http://wrap.warwick.ac.uk/2949/.

Dirlik, T., Benasciutti, D., 2021. Dirlik and Tovo-Benasciutti Spectral Methods in Vibration Fatigue: A Review with a Historical Perspective. Metals 11. doi:10.3390/met11091333.

Zanarini, A., 2005a. Damage location assessment in a composite panel by means of electronic speckle pattern interferometry measurements, in: Proceedings of the IDETC/CIE ASME International Design Engineering Technical Conferences & Computers and Information in Engineering Conference, Long Beach, California, USA, September 24-28, ASME. pp. 1–8. doi:10.1115/DETC2005-84631. paper DETC2005-84631.

Zanarini, A., 2005b. Dynamic behaviour carachterization of a brake disc by means of electronic speckle pattern interferometry measurements, in: Proceedings of the IDETC/CIE ASME International Design Engineering Technical Conferences & Computers and Information in Engineering Conference, Long Beach, California, USA, September 24-28, ASME. pp. 273–280. doi:10.1115/DETC2005-84630. paper DETC2005-84630.

Zanarini, A., 2007. Full field ESPI measurements on a plate: challenging experimental modal analysis, in: Proceedings of the XXV IMAC, Orlando (FL) USA, Feb 19-22, SEM. pp. 1–11. URL: https://www.researchgate.net/publication/266896551_Full_field_ESPI_measurements_on_a_plate_Challenging_Experimental_Modal_Analysis. paper s34p04.

Zanarini, A., 2008a. Fatigue life assessment by means of full field ESPI vibration measurements, in: Sas, P. (Ed.), Proceedings of the ISMA2008 Conference, September 15-17, Leuven (Belgium), KUL. pp. 817–832. doi:10.13140/RG.2.1.3452.9365. Condition monitoring, Paper 326.

Zanarini, A., 2008b. Full field ESPI vibration measurements to predict fatigue behaviour, in: Proceedings of the IMECE2008 ASME International Mechanical Engineering Congress and Exposition, October 31- November 6, Boston (MA) USA, ASME. pp. 165–174. doi:10.1115/IMECE2008-68727. paper IMECE2008-68727.

Zanarini, A., 2014a. On the estimation of frequency response functions, dynamic rotational degrees of freedom and strain maps from different full field optical techniques, in: Proceedings of the ISMA2014 including USD2014 - International Conference on Noise and Vibration Engineering, Leuven, Belgium, September 15-17, KU Leuven. pp. 1177–1192. URL: http://past.isma-isaac.be/downloads/isma2014/papers/isma2014_0676.pdf. Dynamic testing: methods and instrumentation, paper ID676.

Zanarini, A., 2014b. On the role of spatial resolution in advanced vibration measurements for operational modal analysis and model updating, in: Proceedings of the ISMA2014 including USD2014 - International Conference on Noise and Vibration Engineering, Leuven, Belgium, September 15-17, KU Leuven. pp. 3397–3410. URL: http://past.isma-isaac.be/downloads/isma2014/papers/isma2014_0678.pdf. Operational modal analysis, paper ID678.

Zanarini, A., 2015a. Accurate FRFs estimation of derivative quantities from different full field measuring technologies, in: Proceedings of the ICoEV2015 International Conference on Engineering Vibration, Ljubljana, Slovenia, September 7-10, Univ. Ljubljana & IFToMM. pp. 1569–1578. URL: https://www.researchgate.net/publication/280013778_Accurate_FRF_estimation_of_derivative_quantities_from_different_full_field_measuring_technologies. ID192.

Zanarini, A., 2015b. Comparative studies on full field FRFs estimation from competing optical instruments, in: Proceedings of the ICoEV2015 International Conference on Engineering Vibration, Ljubljana, Slovenia, September 7-10, Univ. Ljubljana & IFToMM. pp. 1559–1568. URL: https://www.researchgate.net/publication/280013709_Comparative_studies_on_Full_Field_FRFs_estimation_from_competing_optical_instruments. ID191.

Zanarini, A., 2015c. Full field experimental modelling in spectral approaches to fatigue predictions, in: Proceedings of the ICoEV2015 International Conference on Engineering Vibration, Ljubljana, Slovenia, September 7-10, Univ. Ljubljana & IFToMM. pp. 1579–1588. URL: https://www.researchgate.net/publication/280013788_Full_field_experimental_modelling_in_spectral_approaches_to_fatigue_predictions. ID193.

Zanarini, A., 2015d. Model updating from full field optical experimental datasets, in: Proceedings of the ICoEV2015 International Conference on Engineering Vibration, Ljubljana, Slovenia, September 7-10, Univ. Ljubljana & IFToMM. pp. 773–782. URL: https://www.researchgate.net/publication/280013876_Model_updating_from_full_field_optical_experimental_datasets. ID196.

Zanarini, A., 2018. Broad frequency band full field measurements for advanced applications: Point-wise comparisons between optical technologies. Mechanical Systems and Signal Processing 98, 968 – 999. doi:10.1016/j.ymssp.2017.05.035.

Zanarini, A., 2019a. Competing optical instruments for the estimation of Full Field FRFs. Measurement 140, 100 – 119. doi:10.1016/j.measurement.2018.12.017.

Zanarini, A., 2019b. Full field optical measurements in experimental modal analysis and model updating. Journal of Sound and Vibration 442, 817 – 842. doi:10.1016/j.jsv.2018.09.048.

Zanarini, A., 2020. On the making of precise comparisons with optical full field technologies in NVH, in: ISMA2020 including USD2020 - International Conference on Noise and Vibration Engineering, Leuven, Belgium, September 7-9, KU Leuven. pp. 2293–2308. URL: https://past.isma-isaac.be/downloads/isma2020/proceedings/Contribution_695_proceeding_3.pdf. Optical methods and computer vision for vibration engineering, paper ID 695.

Zanarini, A., 2022a. About the excitation dependency of risk tolerance mapping in dynamically loaded structures, in: ISMA2022 including USD2022 - International Conference on Noise and Vibration Engineering, Leuven, Belgium, September 12-14, KU Leuven. pp. 3804–3818. URL: https://past.isma-isaac.be/downloads/isma2022/proceedings/Contribution_208_proceeding_3.pdf. paper ID 208 in Vol. Structural Health Monitoring.

Zanarini, A., 2022b. Chasing the high-resolution mapping of rotational and strain FRFs as receptance processing from different full-field optical measuring technologies. Mechanical Systems and Signal Processing 166, 108428. doi:10.1016/j.ymssp.2021.108428.

Zanarini, A., 2022c. Introducing the concept of defect tolerance by fatigue spectral methods based on full-field frequency response function testing and dynamic excitation signature. International Journal of Fatigue 165, 107184. doi:10.1016/j.ijfatigue.2022.107184.

Zanarini, A., 2022d. On the approximation of sound radiation by means of experiment-based optical full-field receptances, in: ISMA2022 including USD2022 - International Conference on Noise and Vibration Engineering, Leuven, Belgium, September 12-14, KU Leuven. pp. 2735–2749. URL: https://past.isma-isaac.be/downloads/isma2022/proceedings/Contribution_207_proceeding_3.pdf. paper ID 207 in Vol. Optical Methods.

Zanarini, A., 2022e. On the defect tolerance by fatigue spectral methods based on full-field dynamic testing. Procedia Structural Integrity 37, 525–532. doi:10.1016/j.prostr.2022.01.118. paper ID 105, ICSI 2021 The 4th International Conference on Structural Integrity.

Zanarini, A., 2022f. On the exploitation of multiple 3D full-field pulsed ESPI measurements in damage location assessment. Procedia Structural Integrity 37, 517–524. doi:10.1016/j.prostr.2022.01.117. paper ID 104, ICSI 2021 The 4th International Conference on Structural Integrity.

Zanarini, A., 2023a. Experiment-based optical full-field receptances in the approximation of sound radiation from a vibrating plate, in: IMAC XLI - International Modal Analysis Conference - Keeping IMAC Weird: Traditional and Non-traditional Applications of Structural Dynamics, Austin (Texas), USA, Springer Nature Switzerland AG & SEM Society for Experimental Mechanics. pp. 1–13. doi:10.1007/978-3-031-34910-2_4. paper ID 14650 - chapter 4, in J. Baqersad, D. Di Maio (eds.), Computer Vision & Laser Vibrometry, Volume 6, Conference Proceedings of the Society for Experimental Mechanics Series.

Zanarini, A., 2023b. On the influence of scattered errors over full-field receptances in the Rayleigh integral approximation of sound radiation from a vibrating plate. Acoustics 5, 948–986. URL: https://www.mdpi.com/2624-599X/5/4/55, doi:10.3390/acoustics5040055.

Zanarini, A., 2023c. Risk tolerance mapping in dynamically loaded structures as excitation dependency by means of full-field receptances, in: IMAC XLI - International Modal Analysis Conference - Keeping IMAC Weird: Traditional and Non-traditional Applications of Structural Dynamics, Austin (Texas), USA, Springer Nature Switzerland AG & SEM Society for Experimental Mechanics. pp. 43–56. doi:10.1007/978-3-031-34910-2_9. paper ID 14648 - chapter 9, in J. Baqersad, D. Di Maio (eds.), Computer Vision & Laser Vibrometry, Volume 6, Conference Proceedings of the Society for Experimental Mechanics Series.

Zorman, A., Slavič, J., Boltežar, M., 2023. Vibration fatigue by spectral methods—a review with open-source support. Mechanical Systems and Signal Processing 190, 110149. doi:10.1016/j.ymssp.2023.110149.